



HAL
open science

Numerical modelling for earthquake engineering: the case of lightly RC structural walls

Jacky Mazars, Frédéric Ragueneau, Géraldine Casaux, Antonella Colombo,
Panagiotis Kotronis

► To cite this version:

Jacky Mazars, Frédéric Ragueneau, Géraldine Casaux, Antonella Colombo, Panagiotis Kotronis. Numerical modelling for earthquake engineering: the case of lightly RC structural walls. *International Journal for Numerical and Analytical Methods in Geomechanics*, 2004, 28 (7-8), pp.857-874. <10.1002/nag.363>. <hal-01007124>

HAL Id: hal-01007124

<https://hal.science/hal-01007124v1>

Submitted on 28 May 2024

HAL is a multi-disciplinary open access archive for the deposit and dissemination of scientific research documents, whether they are published or not. The documents may come from teaching and research institutions in France or abroad, or from public or private research centers.

L'archive ouverte pluridisciplinaire HAL, est destinée au dépôt et à la diffusion de documents scientifiques de niveau recherche, publiés ou non, émanant des établissements d'enseignement et de recherche français ou étrangers, des laboratoires publics ou privés.



HAL Authorization

Numerical modelling for earthquake engineering: the case of lightly RC structural walls

J. Mazars¹, F. Ragueneau², G. Casaux², A. Colombo¹ & P. Kotronis¹

*¹Laboratoire Sols, Solides, Structures (L3S), RNVO network
Domaine Universitaire BP 53, 38041 Grenoble cedex 9, France
Tel. +33 (0)4 76 82 51 75
Fax. +33 (0)4 76 82 70 00*

*²Laboratoire de Mécanique et de Technologie (LMT)
61, av. du Président Wilson, 94230 Cachan, France
Tel. +33 (0)1 47 40 53 69
Fax. +33 (0)1 47 40 74 60*

Abstract

Different types of numerical models exist to describe the non-linear behaviour of reinforced concrete structures. Based on the level of discretisation they are often classified as refined or simplified ones. The efficiency of two simplified models using beam elements and damage mechanics in describing the global and local behaviour of lightly reinforced concrete structural walls subjected to seismic loadings is investigated in this paper. The first model uses an implicit and the second an explicit numerical scheme. For each case, the results of the CAMUS 2000 experimental program are used to validate the approach.

Keywords: reinforced concrete, damage mechanics, beam elements, simplified analysis.

Introduction

Reinforced concrete (R/C) bearing walls with limited reinforcement are often used in France and other European countries. Recent experimental programs (e.g. CASSBA, CAMUS) have showed that this type of structural element exhibits good behaviour under seismic loading, although its ductility might be limited due to the light reinforcement and the existence of large sections in the walls with practically no steel [1]. Some unconventional mechanisms of earthquake resistance have also been highlighted such as rigid block-type rotations of the walls (at the interface between the foundation and the soil or at the level of construction joints) or the excitation of high frequency vibrations corresponding to pumping vertical motions (due to the opening and closing of wide horizontal cracks and the conversion of part of the seismic into potential energy). Furthermore, in case of an out of plane loading additional fluctuation of the axial force may arise and heavy damage is expected since cracks do not completely close at load reversal. It is therefore easily understood that the conventional elastic seismic analysis is not adequate to take into account all these effects. More reliable numerical tools are necessary to assist engineers during the design phase.

Various modelling strategies have been proposed up to now for the non-linear analysis of R/C structures. Their level of complexity is usually proportional to the dimension of the problem. Detailed 2D or 3D finite element models with local constitutive relationships are typically used for predicting the response of structural elements or substructures, whereas simplified global or local models are useful for the dynamic response analysis of structures. In this paper the performance of two simplified models - a fibre model and a beam model with multiple integration points - is evaluated using the experimental results of two five-

storey lightly R/C walls subjected to dynamic loading. Both models use local constitutive laws based on damage mechanics and plasticity. The use of an implicit (for the fibre model) and an explicit numerical scheme (for the beam model) is also investigated.

The CAMUS 2000 research program

The 3-years experimental and numerical research program CAMUS 2000 was launched in 1998 with the aim of evaluating the effects of torsion and the behaviour of lightly R/C walls subjected to bi-directional motions [2]. The design of the mock-ups was made according to the "multifuse" concept commonly used in France that privileges diffuse rupture at several stories instead of concentration at the base of the building with the creation of one plastic hinge. Low percentages of reinforcement combined with an appropriate distribution at several levels helps to dissipate energy via wide crack patterns at different heights of the wall and leads into multiplication of the dissipation zones [3].

Two 1/3rd scaled models were tested on the Azalée shaking table of Commissariat à l'Energie Atomique (C.E.A.) in the Saclay Nuclear Centre. The specimens were composed of two parallel braced walls linked with 6 square slabs. A highly reinforced footing allowed the anchorage to the shaking table. Two shear walls in one direction and a steel bracing system in the orthogonal direction provided structural stiffness. Due to similarity laws additional masses of 6.55 tons were positioned at each story. The first structure (CAMUS 2000-1) was subjected to a horizontal bi-directional excitation (Figure 1). A set of accelerograms of increasing amplitude (0.15g, 0.22g, 0.25g, 0.40g, 0.55g and 0.65g) was applied to the specimen. The accelerograms were modified in time according to the ratio $1/\sqrt{3}$ to account for similarity rules. For the second test (CAMUS 2000-2) only an in

plane excitation was applied. The torsional response was caused by the dissymmetry in the horizontal dimensions of the two walls (Figure 2). The distribution of reinforcement for both specimens is described in Tables 1 and 2.

Fibre model (implicit procedure)

1. Numerical tools

Non-linear dynamic analysis of civil engineering buildings requires large-scale calculations and the use of delicate solution strategies. The response of a structure subjected to severe loading depends on a strong interaction between "material" (plasticity, cracks), "structural" (geometry, mass distribution, construction joints) and "environmental" effects (boundary conditions, soil – structure interaction). The major sources of non-linearity for a R/C structure are often on the "material" level. In order to reproduce correctly the main physical phenomena at this level (damage, permanent strain, crack-reclosure) one has to use advanced local constitutive relationships. For the structural level however, a "simplified approach" helps to reduce the computational cost and facilitates parametrical studies.

The choice of a multifibre finite element configuration combines the advantage of using Bernoulli beam type finite elements with 1D local constitutive laws. Each finite element is a beam discretized into several fibres where different material properties can be assigned (Figure 3). In case where shear deformations are prevailing the Timoshenko beam theory can also be adopted [4]. For the general 3D case the cross section behaviour - the relation between the generalized strains \mathbf{e} and the generalized stresses \mathbf{s} - becomes:

$$\mathbf{s} = K_s \mathbf{e}$$

(1)

$$\mathbf{s} = (N \quad S_y \quad S_z \quad M_x \quad M_y \quad M_z)^T \quad \text{and}$$

$$\mathbf{e} = (\varepsilon \quad \gamma_y \quad \gamma_z \quad \theta_x \quad \chi_y \quad \chi_z)^T$$

where N is the normal force, S_y et S_x the shear forces, M_x the torque, M_y and M_z the bending moments, ε the axial strain, θ_x the twist, χ_y and χ_z the curvatures. The matrix

K_s has the following form [5]:

$$K_s = \begin{bmatrix} K_{s11} & 0 & 0 & 0 & K_{s15} & K_{s16} \\ & K_{s22} & 0 & K_{s24} & 0 & 0 \\ & & K_{s33} & K_{s34} & 0 & 0 \\ & & & K_{s44} & 0 & 0 \\ & & & & K_{s55} & K_{s56} \\ \text{sym} & & & & & K_{s66} \end{bmatrix} \quad (2)$$

where the coefficients are obtained by integrating over the cross section (y and z axes) :

$$\begin{aligned} K_{s11} &= \int_S E dS; \quad K_{s15} = \int_S E z dS; \\ K_{s16} &= -\int_S E y dS; \quad K_{s22} = k_y \int_S G dS \\ K_{s24} &= -k_y \int_S G z dS; \quad K_{s33} = k_z \int_S G dS; \\ K_{s34} &= k_z \int_S G y dS; \quad K_{s44} = \int_S G (k_z y^2 + k_y z^2) dS \\ K_{s55} &= \int_S E z^2 dS; \quad K_{s56} = -\int_S E y z dS; \quad K_{s66} = \int_S E y^2 dS \end{aligned} \quad (3)$$

E and G are the Young's and shear modulus that vary in y and z , k_y and k_z are the shear reduction factors. The chosen modulus can be initial, secant or tangent, depending on the iterative algorithm used to solve the global equilibrium equations. The components of the constitutive matrix are computed by numerical integration according to (3), with one Gauss point per fibre. An implicit numerical scheme using the initial Young's modulus is chosen for the following calculations done with the fibre model.

The non-linear behaviour of the materials is described within the thermodynamic framework for irreversible processes [6]. To model the behaviour of reinforcement bars we choose the classical plasticity theory with a non-linear kinematic hardening in order to reproduce correctly the observed hysteresis loops [7]. The free energy for this model takes the following form:

$$\rho\psi = \frac{1}{2}(\varepsilon - \varepsilon_p) : H : (\varepsilon - \varepsilon_p) + \frac{1}{2}b\alpha : \alpha \quad (4)$$

in which H is the Hooke's elasticity tensor, ε_p is the plastic strain and α the hardening internal variable. The constitutive equations are obtained by derivation:

$$\sigma = \frac{\partial(\rho\psi)}{\partial\varepsilon} = H : (\varepsilon - \varepsilon_p), \quad (5)$$

$$X = \frac{\partial(\rho\psi)}{\partial\alpha} = b\alpha$$

where X is the stress like hardening variable. The latter is used to describe a modified form of the plasticity criterion allowing remaining within the associated plasticity theory:

$$f = J_2(\sigma - X) + \frac{3}{4}aX : X - \sigma_y \leq 0 \quad (6)$$

where a , b and σ_y are material parameters. Due to the particular geometric characteristics of steel bars only a 1D implementation of the model is carried out. The evolution equation has been modified to account for the particular behaviour of reinforcing steel used in civil engineering. Based on the normality rule in an associated framework we have:

$$\dot{\alpha} = -\lambda g(\varepsilon_p^{\max}) \frac{\partial f}{\partial X} \quad (7)$$

$$g(\varepsilon_p^{\max}) = 0 \text{ if } \left| \varepsilon_p^{\max} \right| \leq \varepsilon_p^{\lim} \text{ and}$$

$$g(\varepsilon_p^{\max}) = 1 \text{ if } \left| \varepsilon_p^{\max} \right| > \varepsilon_p^{\lim}.$$

ε_p^{\lim} is a material parameter corresponding to the stress-strain plateau length without hardening. A typical stress-strain curve predicted by this model is given in Figure 4.

The constitutive model for concrete in earthquake engineering ought to take into account some observed phenomena such as decrease in material stiffness due to cracking, stiffness recovery which occurs at crack closure, inelastic strains concomitant to damage and strain rate effects. To account for such complex phenomena we use a damage model with two scalar damage variables - D_1 for damage in tension and D_2 for damage in compression (La Borderie model [8]). Unilateral effect and stiffness recovery (damage deactivation) are also included. Inelastic strains are taken into account thanks to an isotropic tensor. To account for strain rate effects in dynamics, the model has been improved by modifying the evolution laws (as it is usually done for visco-plastic models [9]). The Gibbs free energy of the model can be expressed as:

$$\chi = \frac{\langle \boldsymbol{\sigma} \rangle_+ : \langle \boldsymbol{\sigma} \rangle_+}{2E(1-D_1)} + \frac{\langle \boldsymbol{\sigma} \rangle_- : \langle \boldsymbol{\sigma} \rangle_-}{2E(1-D_2)} + \frac{\nu}{E} (\boldsymbol{\sigma} : \boldsymbol{\sigma} - Tr(\boldsymbol{\sigma}^2)) + \frac{\beta_1 D_1}{E(1-D_1)} f(\boldsymbol{\sigma}) + \frac{\beta_2 D_2}{E(1-D_2)} Tr(\boldsymbol{\sigma}) \quad (8)$$

where β_1 and β_2 are material coefficients, whereas $\langle \cdot \rangle_+$ and $\langle \cdot \rangle_-$ denotes the positive or negative values of the given variable. $f(\boldsymbol{\sigma})$ and σ_f are the crack closure function and the crack closure stress respectively. E is the initial Young's modulus and ν the Poisson ratio.

For a 1D implementation of the model, the total strain is:

$$\varepsilon = \varepsilon^e + \varepsilon^{in} \quad (9)$$

$$\varepsilon^e = \frac{\sigma_+}{E(1-D_1)} + \frac{\sigma_-}{E(1-D_2)}$$

$$\varepsilon^{in} = \frac{\beta_1 D_1}{E(1-D_1)} f(\sigma) + \frac{\beta_2 D_2}{E(1-D_2)}$$

where ε^e is the elastic strain and ε^{in} the inelastic strain. The partition of the stress is obtained as:

$$\begin{cases} \sigma > 0 & \rightarrow \sigma_+ = \sigma, \sigma_- = 0 \\ \sigma < 0 & \rightarrow \sigma_+ = 0, \sigma_- = \sigma \end{cases} \quad (10)$$

Damage criteria are expressed as $f_i = Y_i - Z_i - Y_{0i}$ (i=1 for tension or 2 for compression, Y_i is the associated force to the damage variable D_i and Z_i a threshold depending on the hardening variables). The evolution laws for the damage variables D_i are obtained thanks to normality rules:

$$\dot{D}_i = \dot{\lambda} \frac{\partial f_i}{\partial Y_i} \quad (11)$$

As for visco-plasticity, the plastic multiplier is imposed as function of the threshold criterion,

$$\dot{\lambda} = \frac{1}{m_i} \left(\frac{\langle Y_i - Z_i - Y_{0i} \rangle}{Y_{0i}} \right)^{n_i} \quad (12)$$

where Y_{0i} is the initial elastic threshold and m_i and n_i are parameters to be identified for tension and compression to recover the relative effects of strain rate on the peak stress observed on concrete specimens subject to various dynamic loads.

A typical stress-strain response of the model for a uniaxial cyclic loading (tension, compression) and for two different strain rates is given in Figure 5.

2. Numerical simulation

The finite element mesh used for the calculations is presented in Figure 6. The additional masses and the weight load of each floor are concentrated at each storey. The stiffness of the springs below the shaking table is calibrated to fit the first eigenmodes measured before the application of the seismic loads. The following calculations are done with the finite element code CAST3M developed at C.E.A..

A first series of calculations (modal analysis) is performed to check the ability of the proposed model to reproduce the main characteristics of the CAMUS 2000-1 specimen (boundary conditions, masse distributions). The shaking table has to be included to the mesh (with orthogonal beams) to insure the good correlation of the calculations. The values of the first four eigen frequencies and mode shapes are presented in Figure 7 (fiber model). Comparison with the measured ones shows a good agreement.

Despite the lack of physical meaning, damping is generally introduced in the analysis through viscous forces generated by the means of a damping matrix (the classical viscous Rayleigh damping matrix, derived from the general expression proposed by Caughey [10]). Two parameters – the Rayleigh damping coefficients - allow calibrating the matrix by imposing the value of the damping ratio for two eigenmodes. For the following calculations the Rayleigh damping coefficients have been adjusted to ensure a value of 1 % on the first mode and 2 % on the second mode. It is important for concrete structures - where cracking induces loss of stiffness and shift of the fundamental frequency - to keep these damping

values constant throughout the analysis even during strong non-linear behaviour. Therefore, the damping of the first eigenmode has been chosen so as to remain around the minimum (almost constant) range of the Rayleigh diagram.

Results for the transient dynamic calculations are presented in terms of horizontal top displacements in the plane (X direction) of the walls (Figure 8) and global flexural moment in the Y direction (Figure 9) for the signal corresponding to 0.55g. Tables 3 and 4 allow a comparison between computation and experimental results (global and local quantities) for the CAMUS 2000-1 and CAMUS 2000-2 mock-ups. The results have been obtained without further calibration of the model. Work is in progress on the effects of damping [11] and improvements of the modelling are carried out to account for torsion and 3D material behaviour using an enhanced beam formulation [12].

Beam model (explicit procedure)

1. Numerical tools

Explicit procedures combined with simplified modelling strategies are very useful for solving transient dynamic problems. Taking advantage of the small number of degrees of freedom needed in a simplified modelling strategy, explicit procedures contribute to a significant reduction of the computational cost since they require no iterations and no calculation of the tangent stiffness matrix. Even though they are conditionally stable, this is not always a constraint in Earthquake Engineering because a much smaller time step should be chosen to obtain results that are accurate.

To verify the efficiency of an explicit procedure coupled with a simplified approach in describing the seismic behaviour of R/C wall structures we use a simplified finite element mesh to model the CAMUS 2000-1 specimen. The mesh is realized using 3D beam elements with multiple integration points. It differs from the one presented in the previous paragraphs from the fact that all structural members are characterised by homogeneous cross-sections. The explicit version of the commercial computer code ABAQUS is chosen for the analyses. The description of the mesh follows (Figure 10):

- The structure is modelled using Timoshenko beams. The transverse shear deformation is considered linear elastic, independent of the axial and bending behaviour.
- The sections of the Timoshenko beam elements differ according to the various structural components. More specifically:
 - *Walls.* Beam elements with rectangular section (25 integration points per section) are chosen to model R/C walls. The longitudinal reinforcement is introduced using box section elements (16 integration points per section). The area of the reinforcement bars is transformed into an equivalent area of the box section. Concentrated masses simulate the additional masses placed along the walls.
 - *Slab.* Rectangular and box section elements are used to mesh the slabs. The mass blocks added to the floors to represent the dead load of the structure are modelled using fictive box sections. The density of the material is chosen according to weight of the blocks, whereas the stiffness of the elements is limited in order to avoid their influence on the dynamic behaviour of the structure.

- *Bracing system.* The bracing system is modelled with I section elements (13 integration points per section). The geometry of sections corresponds to the geometry of the steel sections adopted in reality.
 - *Basement.* A network of elements simulates the stiffness of the basement in the three directions. Rectangular section elements are used for concrete and box section elements for reinforcement. The specimen is connected to the table via four circular section beams elements. A preload is applied to these components to reproduce the reality.
 - *Shaking table.* A rigid body composed by rectangular section beams simulates the shaking table. Circular beam elements simulate the compliance of the table. The mass of the table is taken into account through an appropriate material density.
- A lumped mass formulation is adopted.
 - The cross-section of each beam is integrated numerically to obtain the force-moment/strain-curvature relations for the section. In that way a complete generality in material response is achieved, since each point of the section is considered independently by the constitutive routines.

The elastic-plastic model of ABAQUS is chosen to describe the behaviour of steel members. The PRM model simulates the cyclic behaviour of concrete (PRM for Pontiroli-Rouquand-Mazars : [13], [14], [15]). This model distinguishes the behaviour under “traction” and “compression” at the level of a transition zone defined by $(\sigma_{ft}, \varepsilon_{ft})$, where

cracks close (Figure 11 for the cyclic response). In these coordinates, the main equations of the PRM model for an uniaxial loading take the following form :

- Partition of strain and stress tensors:

$$\varepsilon = \varepsilon_d + \varepsilon_{ft} \text{ and } \sigma = \sigma_d + \sigma_{ft} \quad (13)$$

- Constitutive equations (E_0 is the initial Young's modulus) :

$$\text{under traction} \quad (\sigma - \sigma_{ft}) = E_0 \cdot (1-D_t) \cdot (\varepsilon - \varepsilon_{ft}) \quad (14)$$

$$\text{under compression} \quad (\sigma - \sigma_{ft}) = E_0 \cdot (1-D_c) \cdot (\varepsilon - \varepsilon_{ft})$$

D_t is evolved in traction and in compression through the variable $\tilde{\varepsilon} = \sqrt{\langle x \rangle_+^2}$ [13], with $x = \varepsilon$ when load is traction and $x = (\varepsilon - \varepsilon_{ft})$ when load is compression; the maximum value of both evolutions is introduced in the calculation.

D_c evolved through the same variable with $x = \varepsilon$. Then $D_i = \text{fct}(\tilde{\varepsilon}, \varepsilon_{d0}, A_i, B_i)$ with $i = t, c$. $\tilde{\varepsilon}$ drives the damage evolution after the initial threshold ε_{d0} , A_i, B_i are material parameters. $\varepsilon_{ft} = \varepsilon_{ft0}$ (material parameter) when $D_c=0$ and is directly link to D_c afterwards; $\sigma_{ft} = f(\varepsilon_{ft}, D_c)$.

- In order to describe dissipation due to hysteretic loops (Figure 11) a hysteretic stress term is added:

$$\sigma_{\text{hyst}} = (\beta_1 + \beta_2 D_i) E_0 (1-D_i) (\varepsilon - \varepsilon_{ft}) f(\varepsilon - \varepsilon_{ft}) \quad (15)$$

β_1, β_2 are the ‘‘Rayleigh’’ parameters and f is a function used to calibrate the evolution with the strain.

This model has been set up in order to describe 3D situations with an explicit formulation useful for FEM calculation particularly for dynamic loadings. The general 3D formulation of the model relating strain and stress tensors (in bold) is reported below :

$$(\boldsymbol{\sigma} - \boldsymbol{\sigma}_{ft}) = \Lambda_0 (1-D) (\boldsymbol{\varepsilon} - \boldsymbol{\varepsilon}_{ft}) = (1-D) [\lambda_0 \text{trace}(\boldsymbol{\varepsilon} - \boldsymbol{\varepsilon}_{ft})\mathbf{1} + 2\mu_0 (\boldsymbol{\varepsilon} - \boldsymbol{\varepsilon}_{ft})] \quad (16)$$

where $\boldsymbol{\sigma}_{ft}$ and $\boldsymbol{\varepsilon}_{ft}$ are the crack closure stress and strain thresholds used to manage permanent effects; Λ_0 is related to the initial mechanical characteristics. D is issued from a combination of the two modes of damage :

$$D = \alpha_t D_t + (1 - \alpha_t) D_c \quad (17)$$

α_t evolved in between 0 and 1 and the actual values depends on $(\boldsymbol{\varepsilon} - \boldsymbol{\varepsilon}_{ft})$.

The PRM model takes into account crack-closure effects, permanent strains, hysteretic loops and includes in its general form the effects of strain rate. It is formulated in an explicit form, compatible with the use of an explicit algorithm.

2 Numerical simulations for the CAMUS 2001 mock-up

A modal analysis is first carried out in order to check the performance of the model. As it was the case for the fiber model, the material parameters are issued from tests performed on concrete and re-bar samples. The calibration of boundary conditions (footing-support interface) comes from the measurement of the two first natural modes (5.5 Hz and 6.00 Hz for the out-of-plane and the in-plane flexure). Figure 7 shows that the results obtained for the other modes are similar to the ones calculated with the fiber model.

Seven seismic signals of increasing amplitude have been applied during the experimental campaign. Among them, only those corresponding to an intensity of 0.15g,

0.4g and 0.55g are considered in the numerical study. In spite of the simplified approach adopted, numerical and experimental data are in good agreement both at global and at local level. Displacement time histories obtained for 0.4g and 0.55g in the direction parallel to direction of the walls of the CAMUS 2000-1 specimen are shown in Figure 12. A satisfactory agreement between experimental and numerical axial load and moment time histories can also be observed for 0.55g in Figure 13 and Table 5 (maximum values). These results are also comparable to those obtained by the fiber implicit model (Table 3) which confirm the good performance of the beam explicit model.

A complex state of stress inside the walls caused by the combination of bi-directional flexure and shear - similar to that observed during the tests - is also highlighted by the numerical analyses. PRM model allows studying the variation of damage at different points of the section. For example, the damage concentrated at the point TR of the left wall is plotted in Figure 14 (0.55g). The effects of tension and compression are considered separately. It can be observed that the damage due to tension is important at the base of the wall and decreases in the upper stories. On the contrary, compression causes limited damage only in the first story, close to the basement and to the connection with the slab of the first story. That is where the maximum damage occurred during the tests. We can therefore conclude that the simplified approach adopted using a model based on damage mechanics associated to an explicit scheme of resolution is adequate to simulate the response of the CAMUS 2000-1 specimen subjected to a series of severe ground motions.

Conclusions

The dynamic behaviour of two R/C wall buildings tested on a shaking table during the CAMUS 2000 experimental research programme was simulated using two different simplified modelling strategies (a fibre and a beam model) and two resolution schemes (implicit and explicit respectively). The constitutive relationships used for the materials were based on damage mechanics for concrete and plasticity for steel.

Both models were able to reproduce correctly the global response of the structures in terms of maximum values and frequency content. Local phenomena (e.g. elongation of reinforcement bars, concentration of damage) were also qualitatively well simulated. However, in order to reproduce quantitatively all the local phenomena a 3D refined finite element model has to be adopted. A simplified modelling strategy can predict only the general trend of the local indicators. This limited accuracy characterising the results obtained with simplified models is balanced by their reduced computational cost. This aspect takes a fundamental importance when there is a need for parametric studies or vulnerability analyses [16].

Research in progress concerns the validation of the two proposed strategies with a new R/C wall specimen that is going to be tested at the shaking table facility of LNEC in Portugal. Instead of a steel bracing system, a more realistic wall with openings is used this time to provide stiffness in the transversal direction. Finally, research is also undertaken to verify the efficiency of explicit methods and the PRM model for dynamic problems of different nature as the effects of impact of blocks on R/C slabs [17].

REFERENCES

- [1] Mazars, J. 1998. French advanced research on structural walls: An overview on recent seismic programs. *Proceedings of the 11th European Conference on Earthquake Engineering, Invited Lectures*, Paris, CD-ROM.
- [2] Bisch, P. & Coin, A. 2002. The “CAMUS 2000” research. *Proceedings of the 12th European Conference on Earthquake Engineering*, London, CD-ROM.
- [3] PS 92. 1995. Règles de construction parasismique, DTU Règles PS92, AFNOR.
- [4] Kotronis P., Davenne L., Mazars J. 2004. Poutre 3D multifibre Timoshenko pour la modélisation des structures en béton armé soumises à des chargements sévères. *Revue Française de Génie Civil* (accepted for publication).
- [5] Guedes J., Pégon P., Pinto A. 1994. A fibre Timoshenko beam element in CASTEM 2000, special publication Nr. I.94.31, JRC, I-21020 Ispra, Italy.
- [6] Lemaitre J. & Chaboche J.L. *Mechanics of Solids Materials*, Cambridge University Press, 1990.
- [7] Armstrong, P.J & Frederick, C.O. 1966, A Mathematical Representation of the Multiaxial Bauschinger Effect, *G.E.G.B. Report RD/B/N 731*.
- [8] La Borderie, Ch. 1991, Phénomènes unilatéraux dans un matériau endommageable: modélisation et application à l'analyse de structures en béton. *Ph.D. thesis* Univ. Paris 6.
- [9] Dubé, J.F., Pijaudier-Cabot, G., La Borderie, Ch. 1996. Rate Dependent Damage Model For Concrete in Dynamics. *J. Engng. Mech.*, Vol. 122, no. 10, October.
- [10] Caughey T. 1960. Classical normal modes in damped linear systems, *J. Appl. Mech.*, 27, pp. 269-271.

- [11] Mazars J. & Ragueneau F. 2001. Ultimate behavior of R/C bearing walls: experiment and modelling, *ASCE Committee. Reports, Modeling of Inelastic Behavior of RC Structures Under Seismic Loads*, Eds Shing & Tanabé, ISBN 0-7844-0553-0, pp 454-470.
- [12] Casaux G, Ragueneau F., Mazars J. 2003. Multifibre beam element in dynamics : torsional response properties, *VII International Conference on Computational plasticity, COMPLAS 2003*, Eds E.Onate and J.R. Owen, CIMNE, Barcelona.
- [13] Mazars, J. 1986. A Description of Micro- and Macroscale Damage of Concrete Structures, *Engineering Fracture Mechanics*, V.25, No. 5/6.
- [14] Rouquand, A., & Pontiroli, C. 1995. Some Considerations on Implicit Damage Models Including Crack Closure Effects and Anisotropic Behaviour. *Proceedings FRAMCOS-2*, Ed. F.H. Wittmann, AEDIFICATIO Publisher, Freiburg.
- [15] Rouquand, A., & Mazars, J. 2001. Modèle incluant endommagement et dissipation hysteretique couplée, *Internal report CEG –DGA Gramat*, France
- [16] Negro P., & Colombo A. 1998. How Reliable are Global Computer Models? Correlation with Large-Scale Tests. *Earthquake Spectra*, Vol. 14, No. 3, pp. 441-467.
- [17] Mazars J., Berthet-Rambaud Ph., Daudeville L., Nicot Fr. 2002. Rockfall protection: Impact effects on structures. Analysis and modeling, *ISRM International Symposium on Rock Engineering for mountain regions*. Funchal, November 25-28th, Editors Dinis da Gama C. and Ribeiro e Sousa L., Sociedade Portuguesa de Geotecnia.

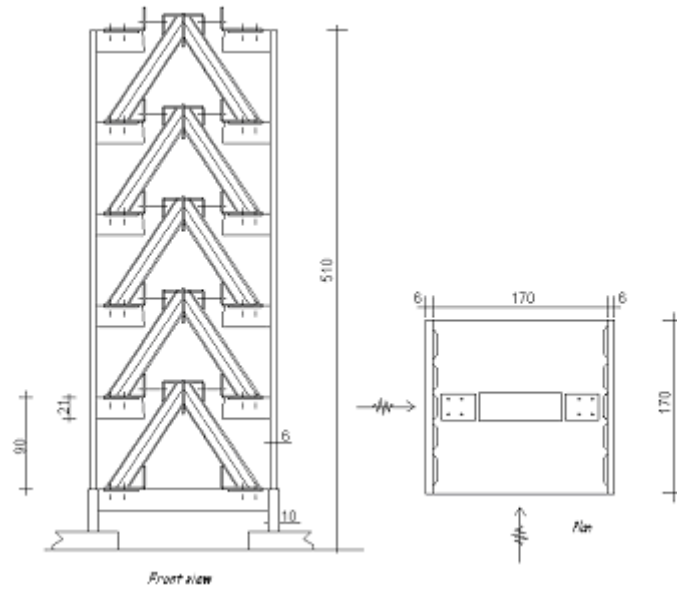


Figure 1. CAMUS 2000-1: Layout of the specimen.



Figure 2. *CAMUS 2000-2*: Non symmetric specimen anchored on the Azalée Shaking table (CEA-Saclay, France).

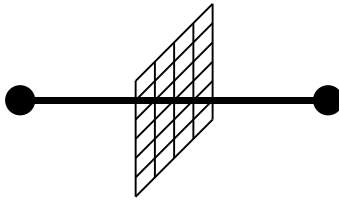


Figure 3. *Multifibre* discretisation principle for a 2-node beam element.

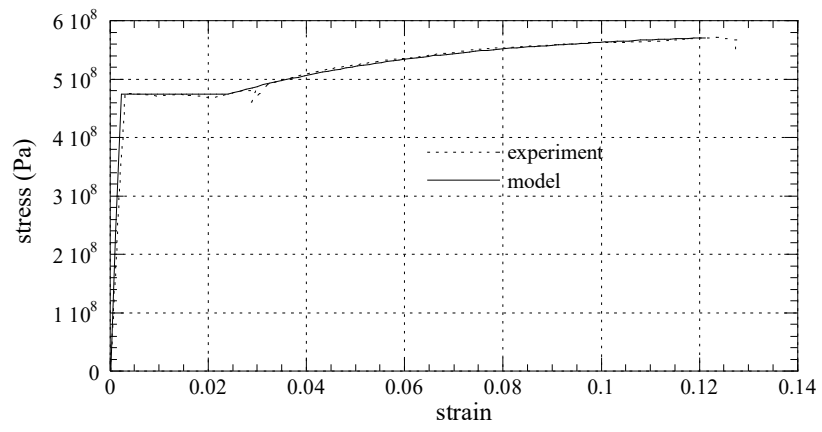


Figure 4 : *Uniaxial steel modeling*. Local model parameter identification.

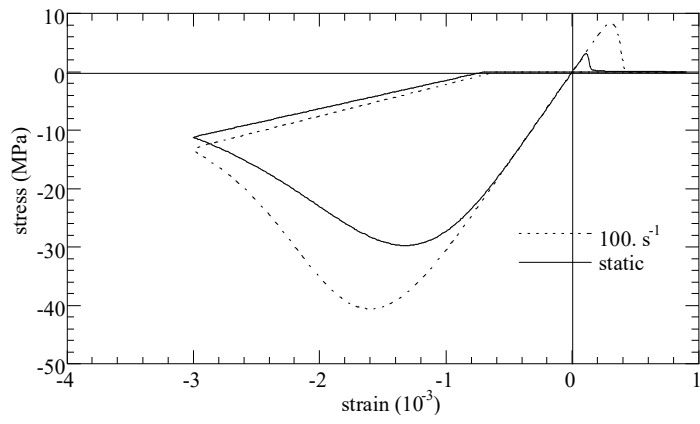


Figure 5. *La Borderie model* : Uniaxial constitutive relations for concrete. Strain rate effects in tension and compression.

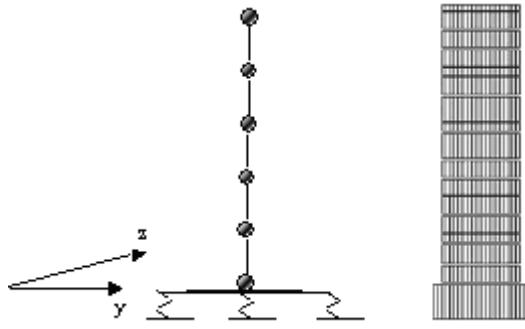


Figure 6 : *CAMUS 2000-1 fiber model*: Finite element mesh.

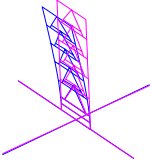
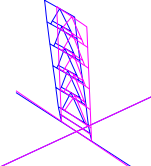
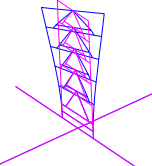
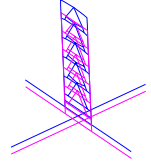
Mode	In-plane flexion	Out of plane flexion	Torsion	Pumping (vertical mode)
Shape				
Experiment	6.0 Hz	5.45 Hz	-	-
Computation				
Fiber model	6.0 Hz	5.5 Hz	10.5 Hz	17.2 Hz
Beam model	6.02 Hz	5.5 Hz	12.56 Hz	19.63 Hz

Figure 7. *CAMUS 2000-1*: Natural eigen frequencies and mode shapes.

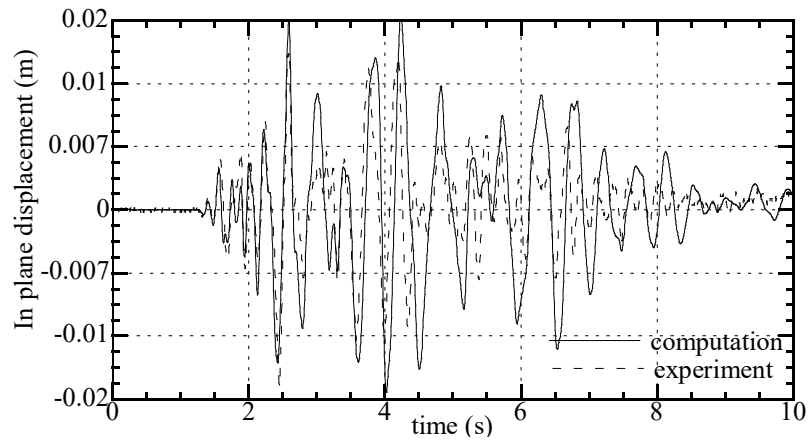


Figure 8. *CAMUS 2000-1 fiber model* : In plane top horizontal displacement (0.55g).

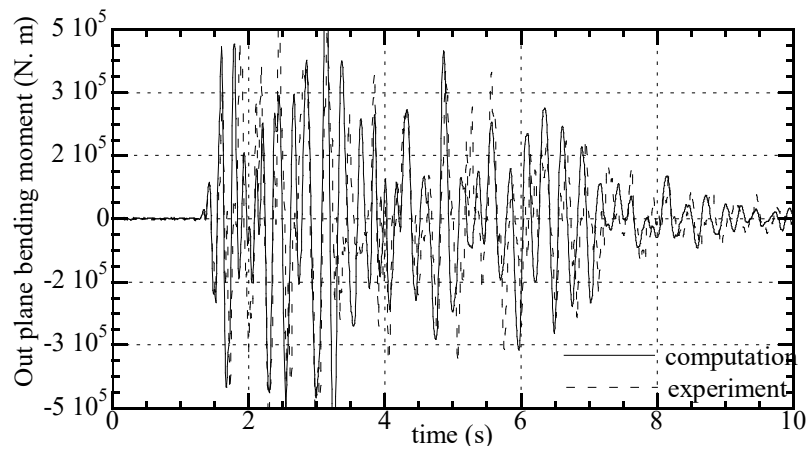


Figure 9. *CAMUS 2000-1 fiber model* : Out of plane bending moment (0.55g).

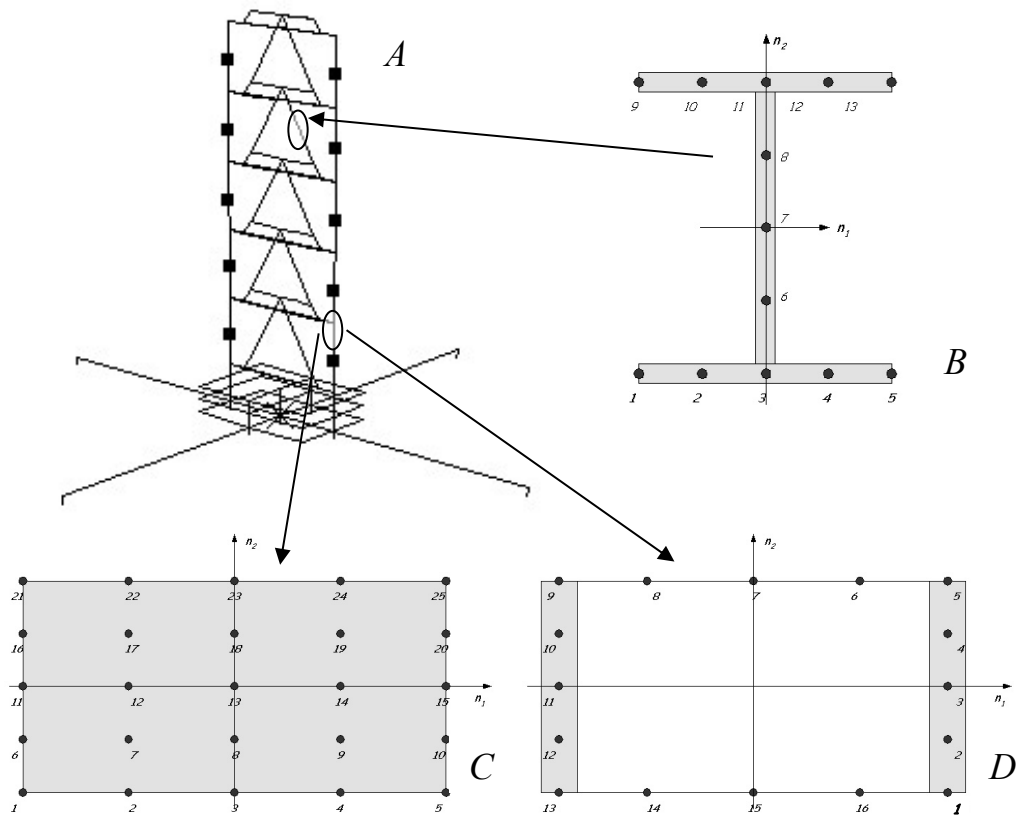


Figure 10. *CAMUS 2000-1: Simplified beam model.* A) Finite element mesh; B) Section shape adopted to model the bracing system; C) Rectangular section element for concrete members; D) Box section used to model the reinforcement and the mass blocks on the floors. Position and number of the integration points in each section are also indicated.

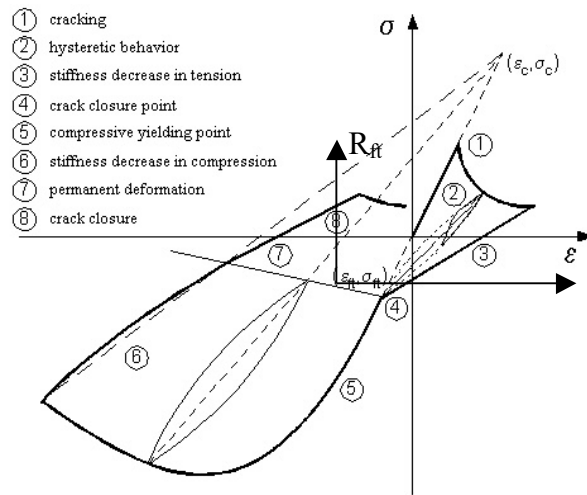


Figure 11. *PRM model*: Uniaxial stress-strain relationship.

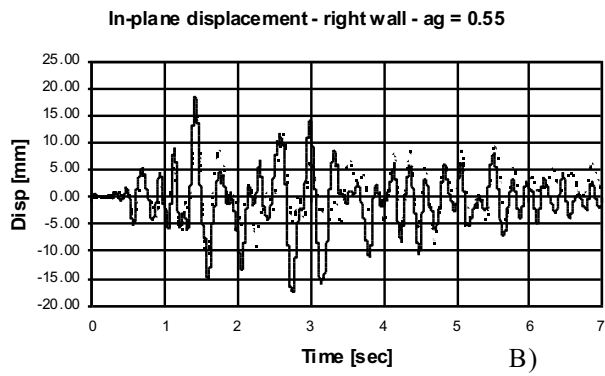
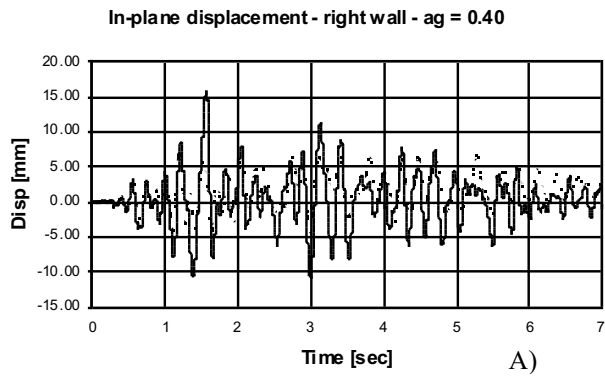


Figure 12. *CAMUS 2000-1 Beam model* : Comparison between calculated (dotted line) and measured (solid line) horizontal top in plane displacements: A) 0.4g B) 0.55g.

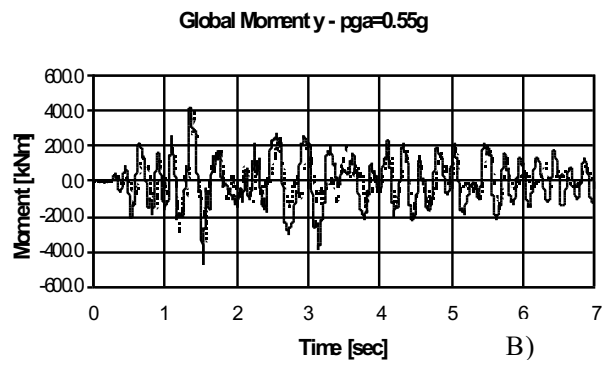
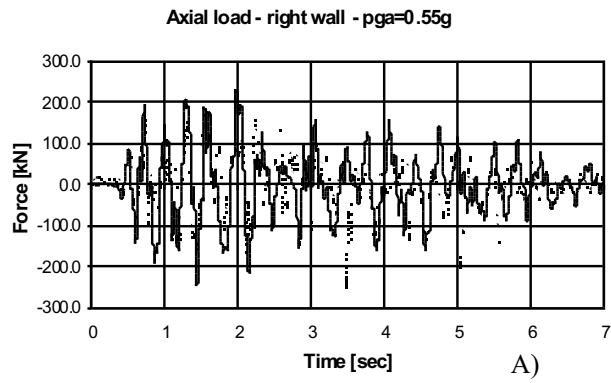


Figure 13. *CAMUS 2000-1 beam model* : Comparison between calculated (dotted line) and measured (solid line) A) axial load in the right wall B) moment at the base of the walls for 0.55g.

TABLE 1. *CAMUS 2000-1*: Reinforcement areas (cm²).

	Floor 1	Floor 2	Floor 3	Floor 4	Floor 5
Reinforcement areas	0,95	0,48	0,16	0,16	0,16
	0,79	0,32			
	0,64	0,16			
	0,48				

TABLE 2 *CAMUS 2000-2*: Reinforcement areas.

Wall	Floor	Reinforcement areas (cm ²)
1,30m x 0,06m	1st	4,15
	2nd	2,86
	3rd	1,57
	4th	0,78
	5th	0,16
2,10m x 0,06m	1st	1,64
	2nd	1,48
	3rd	1,00
	4th	0,50
	5th	0,28

TABLE 3 *CAMUS 2000-1 fiber model* : Numerical versus experimental results.

PGA	<i>0,15 g</i>		<i>0,40 g</i>		<i>0,55 g</i>		<i>0,65 g</i>	
Comparisons	Comp.	Exp.	Comp.	Exp.	Comp.	Exp.	Comp.	Exp.
Left Wall In-plane Disp.(mm)	4,92	4,08	12,9	13,2	22,4	18,7	26,9	31,0
Right Wall In-plane Disp.(mm)	4,40	4,31	15,7	16,1	20,6	18,3	29,5	40,3
Out of plane Disp.(mm)	+3,58 -3,99	+4,93 -4,56	+9,82 -11,8	+12,8 -14,3	+12,4 -18,1	+27,9 -21,5	+12,3 -22,4	+45,7
In-plane Moment(kN.m)	293	225	382	362	452	473	392	407
Out of plane moment	305	331	545	492	649	578	621	500
Left Wall Vertical load (kN)	-	-	-	-	+46,9 -484	+79 -467	+9 -470	+28 -401

TABLE 4 *CAMUS 2000-2 fiber model*: Numerical versus experimental results.

PGA	<i>0,80 g</i>		<i>1,12 g</i>	
Comparisons	Comp.	Exp.	Comp.	Exp.
Left Wall In-plane Displacement (mm)	34,2	32,4	65,2	57,9
Right Wall In-plane Displacement (mm)	33,6	31,8	64,8	63,4
Out of plane displacement (mm)	10,0	6,0	16,4	17,9
Out of plane moment, wall 130 (kN.m)	348	469	393	519
In-plane moment, wall 210 (kN.m)	458	727	503	632
Total axial force, wall 130 (kN)	-8,5	+36	-36,2	+64
	-301	-296	-321	-444
Total axial force, wall 210 (kN)	-52,6	-64	-57	+13
	-303	-278	-335	-398

TABLE 5 *CAMUS 2000-1 Beam Model* : Numerical versus experimental results.

PGA	<i>0,40 g</i>		<i>0,55 g</i>	
Comparisons	Comp.	Exp.	Comp.	Exp.
Left Wall In-plane Disp.(mm)	9.2	13,2	16.5	18,7
Right Wall In-plane Disp.(mm)	8.1	16,1	15.4	18,3
Out of plane Disp.(mm)	+8.9 -7.5	+12,8 -14,3	+11.6 -9.9	+27,9 -21,5
In-plane Moment(kN.m)	393	362	445	473
Left Wall Vertical load (kN)	+165 -318	- -	+135 -363	+79 -467